Environmental Modelling and Software 110 (2018) 95–106

Contents lists available at ScienceDirect

Environmental Modelling & Software

journal homepage: www.elsevier.com/locate/envsoft

Adsorption characteristics of layered soil as delay barrier of some organic contaminants: Experimental and numerical modeling

Sana Dardouri*, Jalila Sghaier

UTTPI, National Engineering School of Monastir, Monastir, Tunisia

ARTICLE INFO

Keywords:
Organic pollutant
Capillary barrier
Modeling
Adsorption
Transport

ABSTRACT

To minimize the contaminant migration in the soil, the use of two and three-layer capillary barriers is proposed as an efficient solution. Indeed, the soil can be used as a physicochemical filter for some pollutants. To discuss the effectiveness of layered soil in the reduction of organic pollutant transport, an experimental and numerical model was developed in this study.

The adsorption capacity of the cationic dye, which used as an example of adsorbed organic pollutant, in a soil (sand, clay, silty soil) has been studied in batch and fixed bed column. It was found that the concentration at the column outlet doesn't exceed 4.5% of the initial concentration after 214 days. Due to the presence of a smectite clay layer and three layer capillary barriers, the transport of dye was insignificant because of the high adsorption capacity of clay and silty soil. The experimental results were also confronted with a numerical simulation. A finite element analysis model was employed in this study to predict the coupled process of variably saturated soils by the contaminants transported in runoff.

Experimental and numerical results confirm that the water velocity and the kinetic adsorption are inversely proportional through the two and three layer barrier system.

1. Introduction

The presence of human and industrial waste is the main reason of the soil contamination. This waste is full of chemicals and toxic products that infiltrate into the subsurface soil which leads to the groundwater pollution. There are many chemicals that can pollute water and soil which entail groundwater and soil contamination as a major problem. As with many contaminants such as volatile organic compounds, heavy metals, fertilizers and detergents, dyes have toxic, mutagenic and carcinogenic effects on human health (Malik and Grohmann, 2011; Chen et al., 2011). Some dyes cause soil contamination due to the toxic nature and harmful effects on all constituents of life. For instance, wastewater from textile dyeing has caused an immense pollution problem for both groundwater and soil.

These dyes are used as tracer on soils to detect preferential flow paths from soil surface to aquifers (Stein et al., 1998) or in soil characterization as in the quantification of colloidal matters in soil inasmuch as the dye is up taken by adsorption onto soil particles surface (Flury and wai, 2003). The methylene blue (MB) is one of the most popular dyes used in textile industries and in the coloring of paper, wools, cotton, silk, etc (Kumar et al., 2005). The MB has also been of use in medical applications. It contains an antiseptic propriety against bacterial infection and it is deployed as an antidote for cyanide poisoning (Reddy et al., 2013). This cationic dye can cause a serious damage to the eyes of living beings and can provoke other health problems such as methemoglobinemia (Mall et al., 2005), profuse sweating, nausea and mental confusion (Christie., 2001).

In recent years, many researchers are interested in soil contamination by persistent organic pollutant. Their studies focus on the impact of persistent pollutant on human health (Ferencz and Balog., 2010). Among others, concentrate on the adsorption of MB onto the soil in batch and continuous fixed bed column (Sana and Jalila, 2016; yukselen and Kaya., 2008; Arab et al., 2015; Auta and Hameed., 2014). In order to study the impact and mobility characteristics of MB pollutant, it's necessary to predict their adsorption and transport in porous media and include the factors affecting its migration and accumulation in soil which is a stratified medium. Soil is made up of different layers. Each layer has its own characteristics that make it distinct from all of the other layers. Soil is also a multiphase system, thus the knowledge of the mechanisms and the coupled process associated with contaminant transport in soil is of great significance to deal with the remediation solutions. Layered soil was proposed in this work as a cover to prohibit the organic pollutant infiltration into groundwater. Because of the relatively high costs of traditional covers (Suter et al., 1993), the cover

* Corresponding author.
E-mail address: sanadardouri_en@yahoo.fr (S. Dardouri).

https://doi.org/10.1016/j.envsoft.2018.09.003
Received 8 December 2016; Received in revised form 13 September 2018; Accepted 15 September 2018
Available online 17 September 2018
1364-8152/ © 2018 Elsevier Ltd. All rights reserved.

with capillary barrier effects (CCBE) represents a promising alternative for the soil contamination problem (Aubertin et al., 2009; Khire et al., 2000; Li et al., 2013; Ng et al., 2015; Sadeghi et al., 2014; Mancarella et al., 2012; Predelus et al., 2015).

Harnas et al., 2014 proposed four layer cover systems with dual capillary to strengthen water storage of the cover. A new three layer capillary barrier cover system is proposed by Ng et al. (2015). Indeed, the CCBE is primarily composed of two-layer unsaturated soil system that employs the contrasting unsaturated hydraulic properties between both soils. The experimental and numerical results showed that the three layer capillary barrier cover system performs well under extreme rainfall. The performance of a CCBE is extremely dependent on the soil-particle size. The change in particle sizes of the soils in a CCBE derives a change in the hydraulic properties. The unsaturated hydraulic properties of the soils influenced on the storage capacity of the surface layer and provoke the apparition an amount of infiltration from covers (Khire et al., 2000).

The determination of the unsaturated hydraulic proprieties is primordial in the modeling of water flow and contaminant transport. Whereas, the methods of measuring of these soil retention properties are time consuming, expensive and are not accurate because of spatial and temporal variability of these parameters. Many authors have proposed to minimize the number of Tensiometers to 2 (wessolek et al., 1994; Fujimakia and Inoue, 2003; Schindler et al., 2010) and Simunek et al., 1998 have used only one tensiometer. Several other researchers have resorted to numerical modeling to solve the problem by choosing time-dependent and space variable boundary conditions (Cremer et al., 2016; Kumar et al., 2015).

The problem is difficult because of the complexities and strong heterogeneities of the geological mass. It is therefore essential to know how to explore predictive models in the absence of sufficient information on heterogeneous hydraulic-physical-chemical properties.

Usually, the transport of species is described by Fickian models of advection and dispersion equations (ADE), following deterministic and/or stochastic approaches (Drummond et al., 2014; Rumynin., 2012; Pedretti., 2014).

Advection dispersion equation (ADE) is extensively used to model several physical, chemical and biological phenomena (Abdelkawy et al., 2015; Li et al., 2017; Song et al., 2018). These processes are coupled and include water flow, solute transport and reaction. The advection dispersion equation could solve the transport of solute in unsaturated medium, in heterogeneous porous media (Pandey et al., 2018) and could account for the impact of retardation (and Song et al., 2018).

Nevertheless, the different versions of the ADE model with a delay coefficient do not accurately describe BTCs, especially for long tails (Berkowitz et al., 2006; Cortis et al., 2006). In contrast, the ADE cannot describe the non Fickian transport (or anomalous) (Bijeljic et al., 2013; Neuman and Tartakovsky., 2009).

A modified form of the convection dispersion equation, including a two-site kinetic retention model was used to simulate the transport and retention behavior of some nanomaterials in porous media (Bradford et al., 2003; Liang et al., 2016; Wang et al., 2012; Fang et al., 2013).

Several models have been developed to predict the concentration profile of the dye in-fixed bed column. These models reproduce the experimental data in order to have a description of the adsorption mechanism. Recent studies have proposed the advection dispersion model to describe the dynamic behavior of a dye in fixed bed column (Hethnawi et al., 2017).

The advection dispersion adsorption equation, which is the advection dispersion equation coupled with kinetic adsorption, was carried out to model the transport of MB in a layered medium.

In this study, our goals were (i) to study the adsorption –desorption and transport behavior of MB in three soils in batch and dynamic mode; (ii) to examine the performance of two and three layers capillary barrier cover system under organic pollutant adsorption in fixed bed column; and (iii) to evaluate the ability of models to replicate the observed results of MB adsorption in soils under different experimental conditions. Besides, a sensitivity analysis was carried out to study the influence of mobile-immobile model parameters on the breakthrough curves.

2. Materials and methods

2.1. Soil and solutions

The soils used in this study were collected from an industrial zone in the region of Sousse in Tunisia. The particle size distribution of sand, clay and silty soil and the exchange capacity (CEC) of clay were measured by laser diffraction particle size analyzer (Microtrac S3500) and by the Metson method (AFNOR NF X31-130) respectively. The mineralogy of the clay sample was established by X-ray diffractometer (XPert PRO PANalytical). The hydraulic parameters and the retention curves of three soils were obtained using cell compression and mini disk infiltrometer (Decagon Devices). The reactive dye methylene blue used as adsorbate (basic blue 9, CI 52015) is a cationic dye with a molecular formula $C_{16}H_{18}ClN_3S.3H_2O$ and a molar mass of 373.9 g mol^{-1}. The wavelength of maximum absorbance for MB is 663 nm.

2.2. Batch experiment

Adsorption isotherms and adsorption kinetics experiments were performed to evaluate the adsorption capacity of MB in three materials.

2.2.1. Adsorption isotherms

The adsorption isotherms were performed in a set of glass flasks (60 ml) containing 25 ml of MB solutions with different initial concentrations (0, 5, 6, 10, 14, 20, 25, 40 mg·L^{-1}) and a 0.5 g of adsorbent added to each solution. These MB solutions were kept under stirring speed of 450 rpm for 48 h, to ensure that adsorption equilibrium was reached. Then the supernatants were fitted and centrifuged before the measurement of its absorbance. The absorbance was measured using a UV− vis spectrophotometer (SpectroFlex6100) by monitoring the absorbance changes at wavelength of maximum absorbance (663 nm). The MB concentrations were estimated using a calibration curve obtained by plotting the absorbance against the concentration of the MB solution. The amount of dye adsorbed per unit weight of sample (sand or clay) at equilibrium, q_e (mg·g^{-1}) was calculated as follow:

$$q_e = m(C_e - C_0)/V \quad (1)$$

where C_0 and C_e are the initial concentration and liquid-phase concentrations of dye solution at equilibrium (mg·L^{-1}) respectively, V is the dye volume (L) and m is the mass of the sample (g). The Langmuir (1918) and Freundlich (1906) models are selected to fit the adsorption isotherms. The non linear form of these models is given as follow:

Freundlich model:

$$q_e = k_F(C_e)^{1/n} \quad (2)$$

Langmuir model:

$$q_e = q_m bC_e/(1 + bC_e) \quad (3)$$

k_F: Freundlich isotherm constant [(mg·g^{-1}) (L·mg^{-1}) ((1 – n)/n)]; n: Freundlich exponent; q_m: Langmuir adsorption capacity (mg·g^{-1}); b: Langmuir isotherm constant (L·mg^{-1}).

2.2.2. Adsorption kinetics

For the adsorption kinetics experiments, vials containing 1 g of sample and 20 ml of MB solutions with 150 mg·L^{-1} initial concentration were shaken at 450 rpm for 90 min. At the end of the predetermined time interval, the vials were filtered then centrifuged at *2500* tr·min^{-1}. The supernatant solution was analyzed using UV–visible

spectrophotometer (SpectroFlex6100) to determine the dye concentration. Each experiment was replicated 3 times to verify the reproducibility of the experience.

The adsorption capacity, q_t ($mg \cdot g^{-1}$) was calculated as:

$$q_t = \frac{(C_0 - C_t)V}{m} \quad (4)$$

where q_t is the dye concentration on adsorbent at time t ($mg \cdot g^{-1}$), C_0 and C_t are the concentrations of the MB solution before and after adsorption respectively ($mg \cdot L^{-1}$), V is the volume of MB solution and m is the mass of dry sample (g). There are many types of the pseudo-second order kinetic equation but in the dye adsorption process, the types 1 and 2 describe more the fitting of kinetic models (Wawrzkiewicz and Hubicki, 2009). Thus, the study of pseudo-second order kinetic is limited to types 1 and 2 in this work. The pseudo-first-order kinetics may be expressed as:

$$log\,(q_e - q_t) = \log q_e - \frac{k_1 t}{2.303} \quad (5)$$

The non linear form of pseudo-second-order equation is given as

$$\frac{t}{q_t} = \frac{1}{k_2 q_e^2} + \frac{1}{q_e} \quad (6)$$

2.3. Column experiment

A series of fixed bed column experiments have been performed to determine the MB behavior in unsaturated soil and to study the effect of capillary barrier on MB transport. The column used in the experiments was made with glass and has a dimension of 3.5 cm in diameter and 25 cm in length. The column experiments were conducted at constant flow rate and at initial MB concentration under unsaturated flow conditions. Then the MB was eluted from the column by rainwater flushing. During the experiment, the effluent samples were collected at the column outlet and measured for MB concentration immediately after sampling. The MB concentrations in the column effluents were determined using UV–vis spectrophotometer. The MB breakthrough curves (BTC) were obtained by plotting relative concentrations (C/C_0) versus time (t). (see Table 1)

3. Breakthrough curves modeling

In this study, three approaches have been investigated for data fitting of MB breakthrough curves. These models include Thomas, convection dispersion and mobile-immobile model.

3.1. Thomas model

The Thomas model (Thomas, 1944) assumes that a Langmuir isotherm and second order kinetic fitted well the experimental data. This model has assumed also that adsorption is limited by mass transfer with no axial dispersion is derived and has allowed the calculation of the adsorption rate constant. The equation of Thomas model can be described as:

Table 1
Experimental conditions for column experiments.

	Saturation condition	Media composition	BM initial Concentration ($mg \cdot L^{-1}$)	Flow rate ($ml \cdot min^{-1}$)	Sample height (cm)
Exp A	Unsaturated	Sand	1000	30	25
Exp B	Unsaturated	Layered Soil	1000	30	25
Exp C	Unsaturated	Silty Soil	1000	0.15	10
Exp D	Unsaturated	Layered Soil	100	0.0261	10

$$\frac{C_t}{C_0} = \frac{1}{1 + e^{\left((q_0 m - C_0 \vartheta t)\frac{k_{th}}{\vartheta}\right)}} \quad (7)$$

where k_{th} is Thomas rate constant ($mL \cdot min^{-1} \cdot mg^{-1}$), q_0 is equilibrium adsorption capacity ($mg \cdot g^{-1}$), m is the mass of the adsorbent, C_0 and C_t are the MB concentration in the influent and at time t ($mg \cdot L^{-1}$) and υ is the flow rate ($mL \cdot min^{-1}$).

3.2. Advection–dispersion- adsorption model

A general transport and adsorption model for a porous medium was used to predict dynamic adsorption breakthrough. This model is based on convection dispersion equation (Eq. (8)) for two dimensional flows through a porous bed (Parker and van Genuchten, 1984).

$$\frac{\partial(\theta C)}{\partial t} + \frac{\partial(\rho_b C_p)}{\partial t} + \nabla(-\theta D_L \nabla C + UC) = \sum R + \sum S \quad (8)$$

where C and C_p are the adsorbate concentration in the liquid and solid phase respectively ($kg \cdot m^{-3}$), ρ_b is the bulk density ($kg \cdot m^{-3}$), θ is the bed water content, k_p is the adsorption rate ($m^3 \cdot kg^{-1}$), U is the Darcy velocity ($m \cdot s^{-1}$), R and S are the reaction and D_L is the hydrodynamic dispersion tensor.

The rate of accumulation in the solid phase term ($\frac{\partial C_p}{\partial t}$) was accounted for the following equation

$$\frac{\partial C_p}{\partial t} = \alpha(K_L C(q_m - C_p) - C_p) \quad (9)$$

α is the rate constant (s^{-1}), q_m is the maximum Langmuir adsorption parameter, C_p is the adsorbent capacity ($kg \cdot m^{-3}$) and K_L is the Langmuir adsorption parameter ($m^3 \cdot kg^{-1}$).

Severe incorporation of Richard equation (Eq. (10)) is to describe the Darcy flow through porous media was coupled with advection dispersion –equation. This coupling is through Darcy velocity equation (Eq. (11)). The Richard equation is expressed as follows:

$$(C + S_e S)\frac{\partial H_p}{\partial t} + \nabla(-K\nabla(H_p + D)) = Q_m \quad (10)$$

$$U = K_s k_r \nabla(H_p + D) \quad (11)$$

where H_p is the pressure head (m), C is the specific moisture capacity, S_e represents the effective saturation, S is the storage coefficient, K is the hydraulic conductivity, k_r is the relative permeability, D represents the elevation (m), and Q_m is the fluid source or sink. The unsaturated soil properties were described using the van Genuchten model.

$$K(\theta) = K_s S_e^2 \left[1 - (1 - S_e)^{1/m}\right]^m \quad (12)$$

where m is the Van Genuchten parameter and K_s denotes the hydraulic permeability.

The main problem for unsaturated flow lies in the choice of boundary conditions at the lower base and the upper base of the domain. In addition to the strong dependence of the hydrodynamic parameters (hydraulic conductivity, Darcy velocity, pressure load …), the degree of water saturation (or water content) at the lower and upper limits of the domain varies over time, especially at the beginning of the experiment, and subsequently the parameters $K(\theta)$, $q(\theta)$ and $h(\theta)$ vary as well. To overcome these difficulties, we use three successive and complementary sub-models to make the right choice of boundary conditions that describe the flow regime throughout the experiment. The following flowchart (Fig. 2) explains, further, the proposed methodology for solving the problem and determining the most appropriate boundary conditions.

We begin by developing a first sub-model for the unsaturated flow regime with zero flux conditions on both the lower and upper surfaces of the geometry. To start the flow from the upper surface (second sub-model), the values recorded on the upper surface during the unsaturated phase (first sub-model) are imported as boundary conditions at the upper base until flow start time (flow) followed by pressure

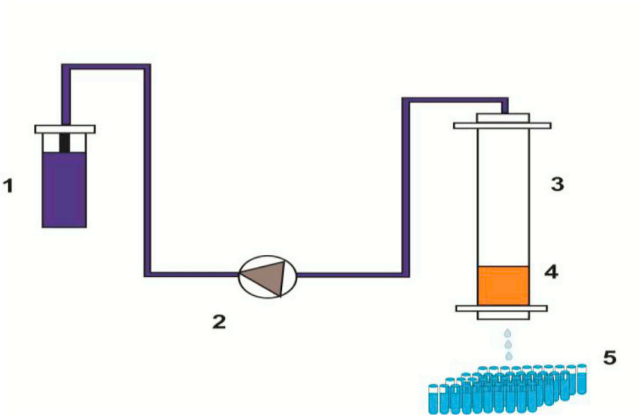

Fig. 1. Schematic of column setup (1. Influent tank; 2. Pump; 3. Column; 4. Adsorbent; 5. Effluent collection).

values imposed by the flow. We keep, for the moment, the zero flow condition at the lower base. The calculation of the second intermediate sub-model is started and the saturation time of the medium is recorded. At this point, the state of saturation of the medium is reached and the pressure load at the bottom surface becomes constant.

Finally, it is the third model that will be the final full model. Provided to the upper surface, is an interpolation function describing the evolution of the capillary pressure taken from the initial time until the time of the start of the flow, followed by the pressure values imposed by the flow. For the condition of the bottom surface, the pressure is the interpolation of the values taken from the initial time until saturation time ($t_{saturation}$) followed by the value of the saturation pressure. The following chart (Fig. 2) can better explain the methodology proposed to solve the problem.

Following the strategy described above for the study of water flow and solute transport in a soil column of height 10 cm and diameter 3.5 cm, the initial and boundary conditions for an unsaturated and saturated medium are described in Fig. 3.

The initial and boundary condition for two dimensional problem used for solving this model are:

$$\begin{cases} C = 0\ \text{kg/m}^3 & t = 0\ \forall\ z \\ C = C_0 & z = 10\ \text{cm} \\ -\,nD_i\nabla C_i = 0 & z = 0\ \text{cm} \end{cases} \tag{13}$$

For the Richard equation, the initial condition is a linear function which describes the pressure head evolution in the column at time 0s. The upper and lower conditions are two interpolation functions (P_1 (t), P_2 (t)) which describe the pressure head evolution at any time throughout the experiment (Fig. 3).

3.3. Mobile-immobile model (MIM)

The transport equation takes into account not only the convection, diffusion and dispersion, but also the phenomenon of retention of the polluting particles by the solid phase of the porous medium via a distribution coefficient K_d. The one-dimensional equation of the MIM transport model for a reactive solute in unsaturated media is (Van Genuchten and Wierenga, 1976):

$$\begin{aligned} &(\theta_m + f\rho_d K_d)\,{}^{\partial C_m}\!/_{\partial t} + (\theta_{im} + (1-f)\rho_d K_d)\,{}^{\partial C_{im}}\!/_{\partial t} \\ &\quad = -q\,{}^{\partial C_m}\!/_{\partial z} + D_m\theta_m\,{}^{\partial^2 C_m}\!/_{\partial z^2} \\ &(\theta_{im} + (1-f)\rho_d K_d)\,{}^{\partial C_{im}}\!/_{\partial t} = K_m(C_m - C_{im}) \end{aligned} \tag{14}$$

where θ_m and θ_{im} represent the mobile and immobile water fractions, respectively, f is the fraction mobile, ρ_d is the bulk density, K_d is the partition coefficient, C_m et C_{im} are the pollutant concentrations in mobile and immobile phase, respectively, D_m is the diffusion coefficient in the fraction mobile and q is the Darcy velocity.

The MIM model parameters are described in the following table: (See Table 2) where D is the diffusion coefficient in Liquid phase, θ is the porosity, λ is the longitudinal dispersivity, ρ is the density, C_o is the initial concentration, K_d is the distribution coefficient, n is the coefficient of Freundlich model and α is the mass transfer coefficient.

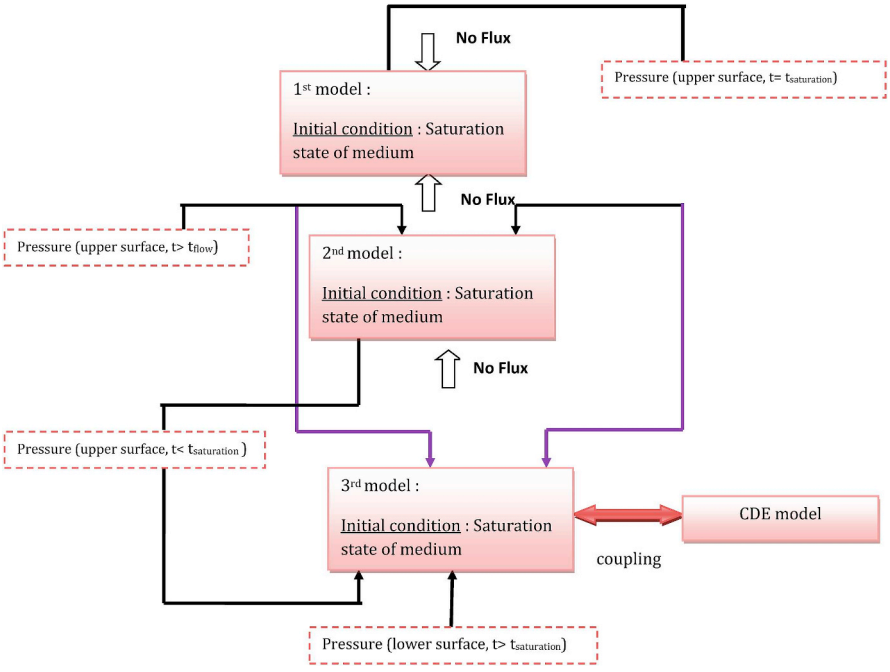

Fig. 2. Code for boundary conditions.

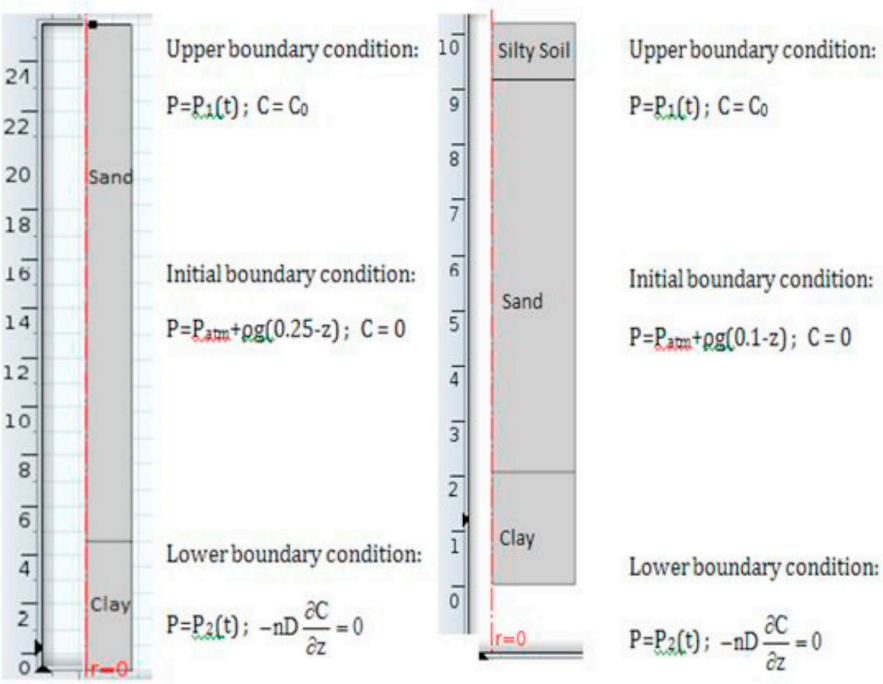

Fig. 3. Geometrie and boundaries conditions for both layered meduim.

Table 2
MIM model parameters.

Parameters	Values
D (cm^2/day)	0.25
λ (cm)	0.1
θ (cm^3/cm^3)	0.48
ρ (g/cm^3)	1.5
C_0 (mmol/l)	0.031
K_d (cm^3/g)	0.27
n	0.823
α (1/day)	0.201

4. Results and discussion

4.1. Samples characterizations

The results of X-Ray spectroscopy show the presence of smectite clay. The smectite clay is characterized by its cationic exchange capacity in the interlayer spaces. The value of this CEC is found to be equal to *90* meq/100 g of clay.

The X-ray diffraction pattern (Fig. 4(a)) had three significant reflections at *15.*6°A, *3.*34°A and 1.45°A.The two reflection distances of *3.*31°A and *1.*45°A indicated the presence of silice and that the clay is a dioctahedral smectite, respectively. The particle size analysis of sand, clay and silty soil samples shows that the fifty percent passing particle size (d_{50}) was calculated as 317 µm and *11.*69 µm based on sieve sizing for sand and clay respectively (Fig. 4(b)). Soil water characteristic curves (θ, h) are presented in the following figure (Fig. 4(c)). Comparing the saturated water content of three soils, we deduce that clay have the high saturated soil water content. The hydrodynamic parameters of three soils are recapitulated in Table 3.

4.2. Adsorption models

It is found that the clay has the best adsorption capacity compared to silty soil and sand. The good fitting of the model with experimental data is represented by a high value of correlation coefficient. For the clay and silty soil adsorbents, the Freundlich model provides a better fit in the MB adsorption isotherm (Fig. 5(b) and (c)). The Freundlich isotherms model predicts multilayer adsorption and describes equilibrium on heterogeneous surfaces (Freundlich, 1906; Gimbert et al., 2008). For sand, modeling of adsorption isotherm shows good agreement with Langmuir (Fig. 5(a)). This model assumes that the forces of interaction between the adsorbed molecules are negligible (Gimbert et al., 2008), there is a single layer of adsorbate on the outer surface of the adsorbent (Langmuir, 1918) and no further adsorption will take place if the molecule occupies the adsorption site.

The prediction of kinetics adsorption is needed to evaluate the adsorption efficiency using both models. The pseudo first order equation represented very well the kinetic data of MB in sand and clay. The applicability of Langmuir isotherm for sand material implies that monolayer adsorption exist under the experimental conditions. The best regression of experimental data for both sand and silty soil is using the type 1 of pseudo second order kinetic equation (Fig. 6(b)).

4.3. Column experiments

4.3.1. Effect of the capillary barrier on MB retention

The Fig. 7 shows the capillary barrier effect on the MB breakthrough curve by comparing homogeneous and layered porous media. This figure clearly shows a difference in the MB behavior during its infiltration in unsaturated homogeneous and layered media (saturated at 60% Vp)). The layered medium (Exp B) consists of *80*% of sand distributed over a height of 20 cm at the top of the column and *20*% clay corresponds to a height of 5 cm. The MB injection is performed at an average flow rate of Q = *8.*5 mL min^{-1} and after a flow stabilization time of 34 min. During the first *60* min, the concentration is zero; the injected solution is pushing the liquid phase initially present in the column. In the layered medium, the MB solution has covered a distance of 20 cm of homogeneous sand then it is found in the contact area between the two layers. This area is a transition zone in which water is trapped for some time to adapt to sudden change in characteristics of the medium. This explains the retardation in the release of the effluent from the column. Then, the concentration gradually increases to a maximum value. This value is equal to C_0 for a homogeneous medium after *319* min while it is equal to *0.88* C_0 for a layered medium after a

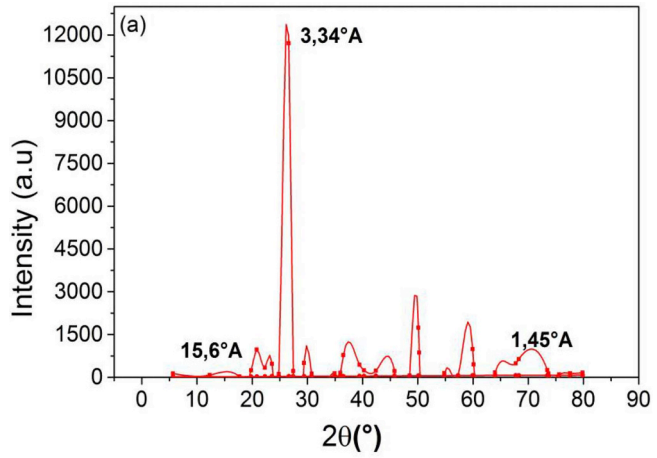

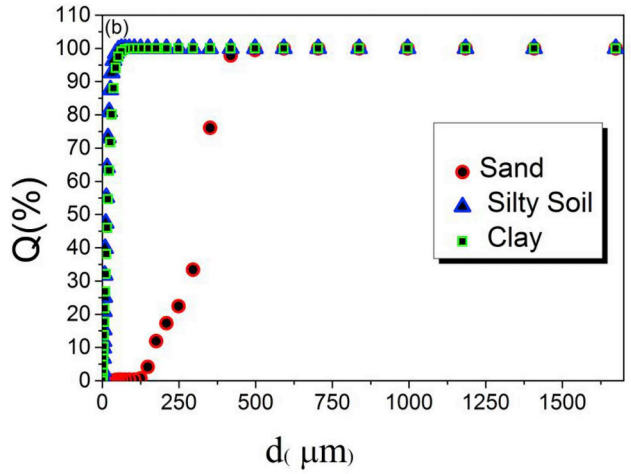

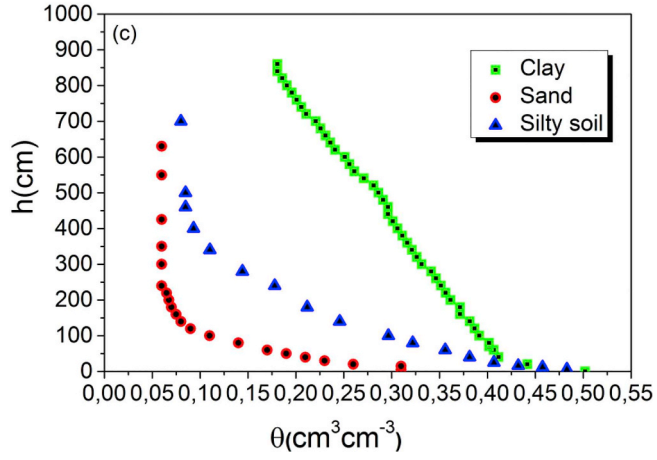

Fig. 4. (a) XRD diagram of smectite clay, (b) Particle size distribution of three soils, (c) retention curves.

time of *578* min. The long tail of the breakthrough curve is due to the MB reactivity with the clay fraction.

4.3.2. Effect of three-barrier system on MB adsorption

The influence of the capillary barrier system on the MB breakthrough curve was also studied using three-layer medium (Fig. 3). The MB concentration increases slowly and depends on the saturation condition and the structure of the porous medium. Indeed, the first

Table 3
Hydrodynamic parameters of soils.

Sand		Clay	Silty Soil
θ_r ($cm^3 \cdot cm^{-3}$)	0.06	0.18	0.0847
θ_s ($cm^3 \cdot cm^{-3}$)	0.31	0.508	0.483
K_s ($m \cdot s^{-1}$)	$2{,}25.10^{-5}$	$3{,}8.10^{-9}$	$5.6.10^{-7}$
α (cm^{-1})	0.02572	0.0483	0.01466
n	2.793	2.0557	2.351

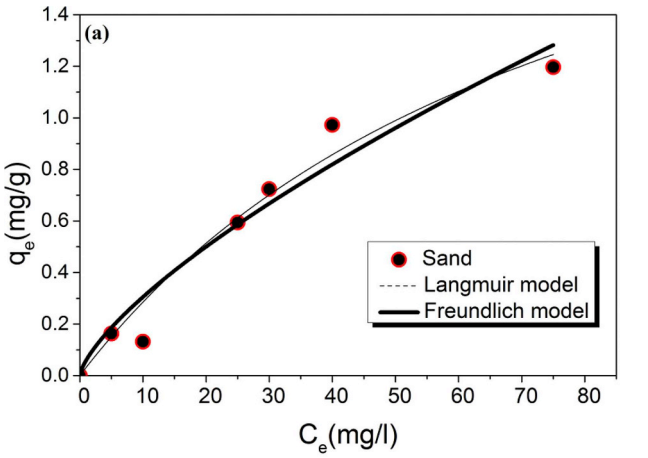

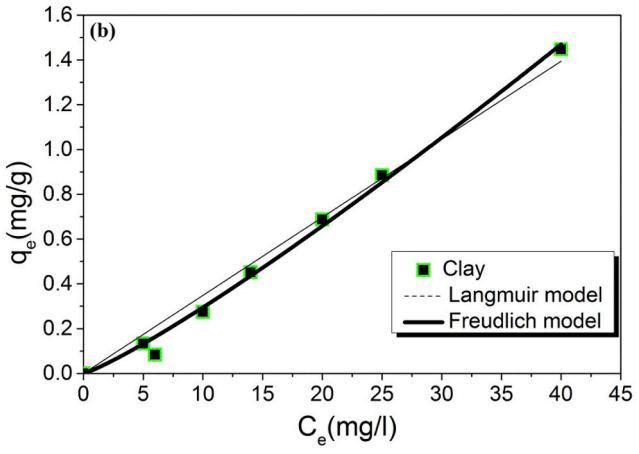

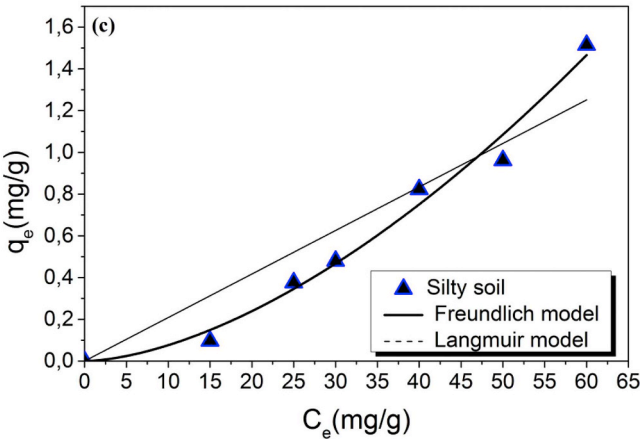

Fig. 5. Adsorption isotherms (a) Sand, (b) Clay, (c) Silty Soil.

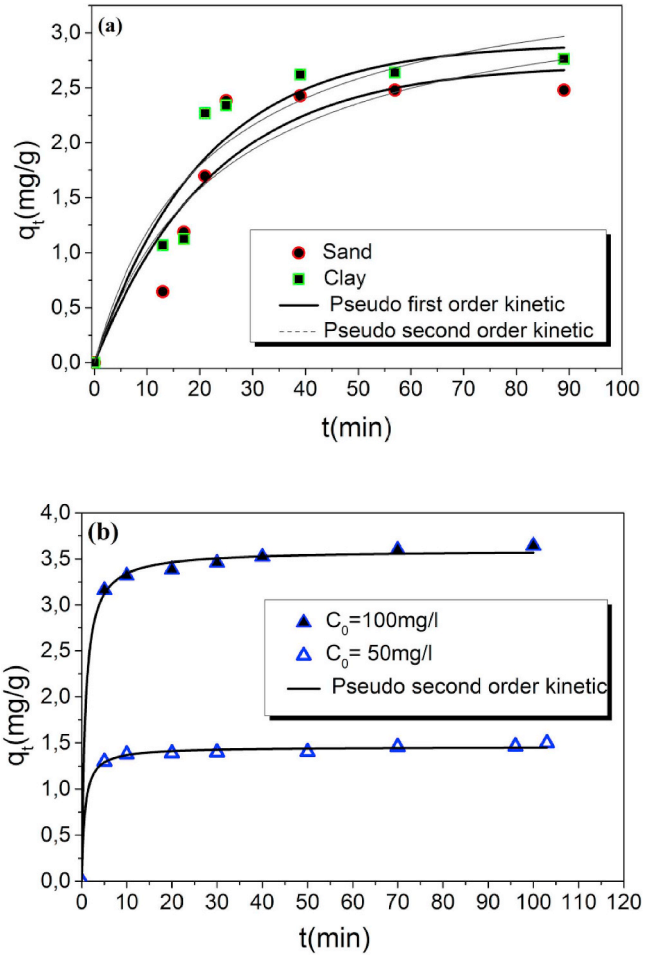

Fig. 6. Kinetic adsorption for (a) sand and clay, (b) Silty soil.

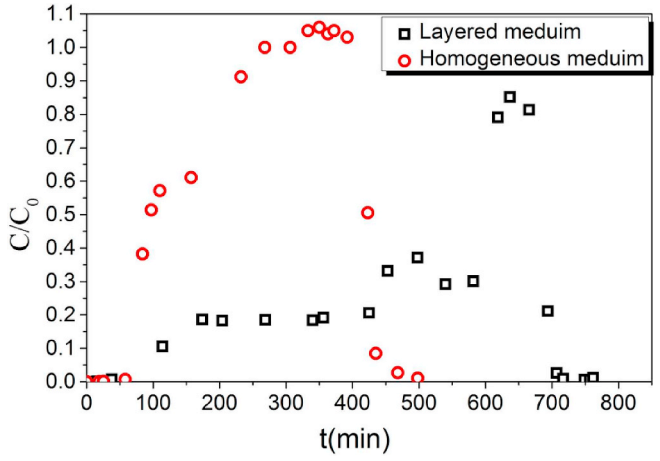

Fig. 7. Comparison homogeneous and layered media (Exp A and Exp B).

layer at the top of the column is a 1 cm of silty soil and the second layer is a 7 cm of sand. Both layers are initially saturated with water. The third layers (2 cm of clay) are initially unsaturated (Exp D). The delay of the MB release (after *104* days) is justified by the physical and chemical heterogeneities of the porous medium. The interface between two porous media having different characteristics is a capillary barrier and a trapping zone. Despite a slight increase in concentration gradient, the steady state of MB transfer is not reached at t = *214* days and outlet concentration does not exceed *4.5*% of the inlet concentration (Fig. 8).

Generally, the BTC in heterogeneous media are described by

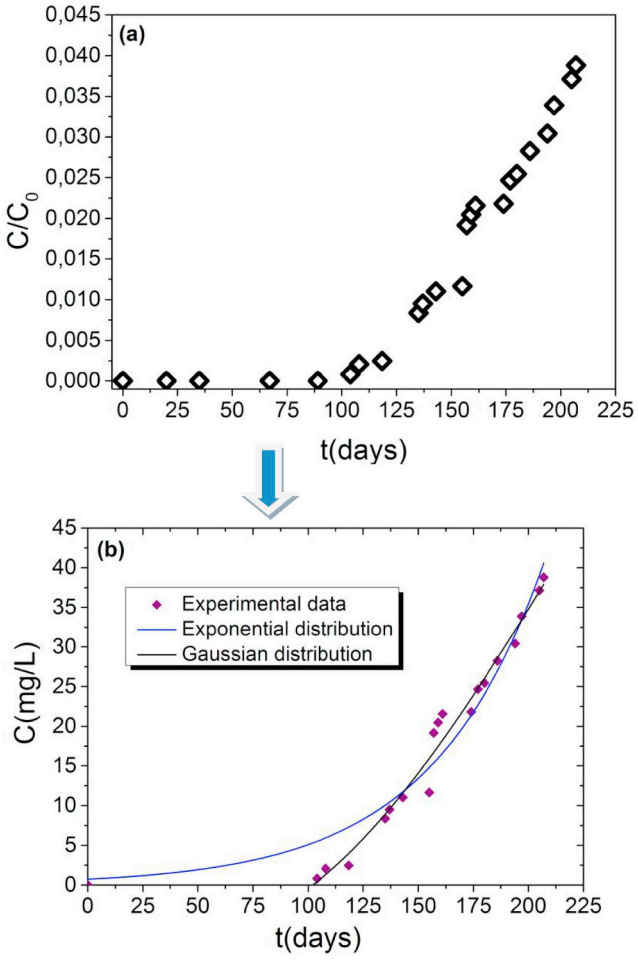

Fig. 8. (a) Breakthrough curve for three layer porous media (Exp D), (b) non linear fitting of BTC.

lognormal distribution and recently this log normal distribution has been endorsed for non-Gaussian correlation (Moslehi and de Barros., 2017). Comparing the exponential distribution (R^2 = *0.94*) and the Gaussian distribution (R^2 = *0.97*), we can conclude that the dispersion process is predominant at the beginning of the curve. The exponential shape of BTC proves that dispersion and sorption are the main processes in the MB transport.

4.4. Models validation

4.4.1. Comparison of Thomas model and convection dispersion adsorption model

A numerical simulation using the advection-dispersion-adsorption model for three layer porous media is carried out. Adsorption is considered linear for silty soil and clay while it is Langmuir type in the sand sample. Eq (8) describes the transport of MB in a porous medium composed of three areas of different physical and chemical properties. These properties are defined in Table 4. The selected geometry is very similar to the physical reality of the experimental setup (Fig. 1). The chosen triangular mesh is refined at the interfaces between the fields and the time step retained during the simulation is 30000s. In Fig. 2 the boundary conditions are described.

For short time (t < *170* days), the convection-dispersion-adsorption model reproduced fairly well the experimental data and for long time (t > *170* days), the numerical curve is well below experimental measurements and the standard error of the simulation with the model Thomas gets weaker (Fig. 9).

Table 4
Parameters, Boundaries and initial conditions of the three layers.

	Silty Soil	Sand	Clay
Advection-dispersion-adsorption equation: Parameters			
Initial saturation	1	1	0.6
Porosity	0.48	0.31	0.5
Adsorption Coefficient	$0.0209\ m^3\ kg^{-1}$	$q_m = 0.0258$ $K_L = 0.18\ m^3\ kg^{-1}$	$0.054\ m^3\ kg^{-1}$
Longitudinal dispersion Coefficient	0.0025 cm		
Diffusion coefficient	$10^{-10}\ m^2\ s^{-1}$		
Bulk density	$1550\ g\ cm^{-3}$	$1{,}4\ g\ cm^{-3}$	$1{,}25\ g\ cm^{-3}$
Initial Conditions	$C = 0\ kg\ m^{-3}$; $Cp = 0$; $\frac{\partial Cp}{\partial t} = 0$		
Advection-dispersion-adsorption equation: Boundary Conditions			
Description	A continuity condition is imposed on all internal boundaries and a maximum concentration of MB is imposed on top of the column. No flow is imposed on the outer boundaries.		

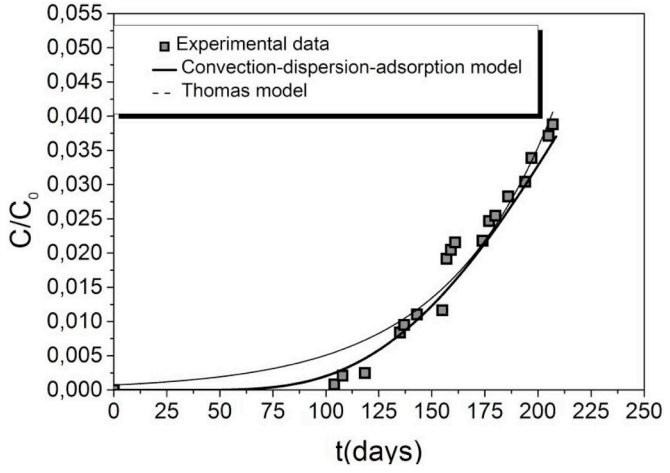

Fig. 9. Comparison of experimental data of MB transport in layered medium with the convection-dispersion-adsorption model and Thomas model.

4.4.2. Kinetic adsorption in layered medium

For the two layer medium and at the interface between the two layers (z = 5 cm), the water is trapped in the capillary barrier composed of two layers (sand and clay), with hydraulic properties are different. This entrapment causes the prevention and accumulation of water at the interface until the water pressure head becomes sufficient to allow it to penetrate (Li et al., 2013). The water pressure gradient increase associated with the accumulation of water in the two media interface has a capillary barrier effect. In this interface, retention is more important (Predelus et al., 2015). Indeed, after *100* min, the adsorbed concentration gradient in $z = 5$ cm (interface between sand and clay materials) is larger compared to homogeneous medium (Fig. 10). This increase in retention capacity at this interface is the result of increase in water content and decreasing in interstitial water velocity, which enhances the trapping of the MB solution (Torkzaban et al., 2008). In fact, the decrease of the pore water velocity is accompanied by a decrease of the adsorption kinetics velocity at the interface (Fig. 11).

The same result is found for a three layers capillary barrier system. The Fig. 12 represents the evolution of adsorption kinetics along the column in the breakthrough time ($t = 8, 64.10^6\ s$) and in the end of the experiment ($t = 1.72.10^7\ s$). Indeed, the adsorption kinetics is increased in two capillary barriers ($z = 9$ cm: interface between silty soil and sand; $z = 2$ cm: interface between sand and clay).

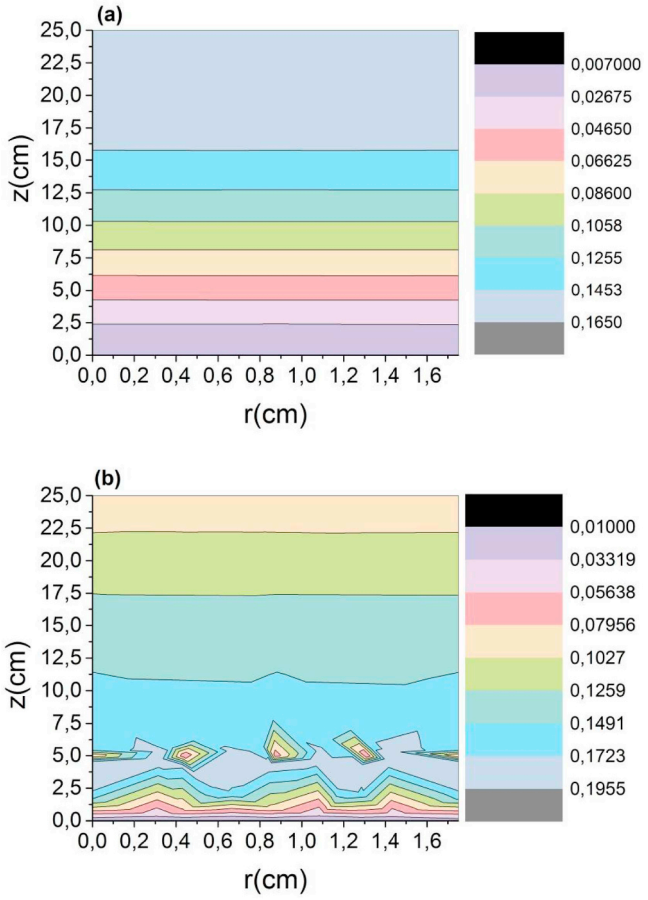

Fig. 10. Evolution of adsorbed concentration gradient (a) in homogeneous medium, (b) in two layer medium.

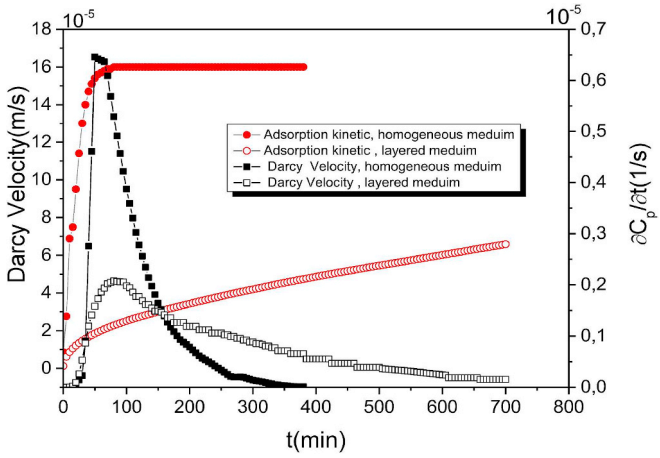

Fig. 11. Evolution of kinetic adsorption and Darcy velocity for homogeneous and two layer media in $z = 5$ cm.

4.4.3. Simulated MB adsorption

Both modeling approaches available in HYDRUS-1D for MB transport were used and compared prior to assisting in the interpretation of the field data. Fig. 12 shows the MB breakthrough curve and model results obtained from the advection–dispersion transport equation, the mobile–immobile solute transport—MIM and Thomas model. The simulated data obtained by the MIM model (Fig. 13) are coherent with experimental data acquired since they prove that MB solution takes 350 h for breaks through a fixed-bed column of 10 cm in height. It is also expected that the shape of the breakthrough curve is not

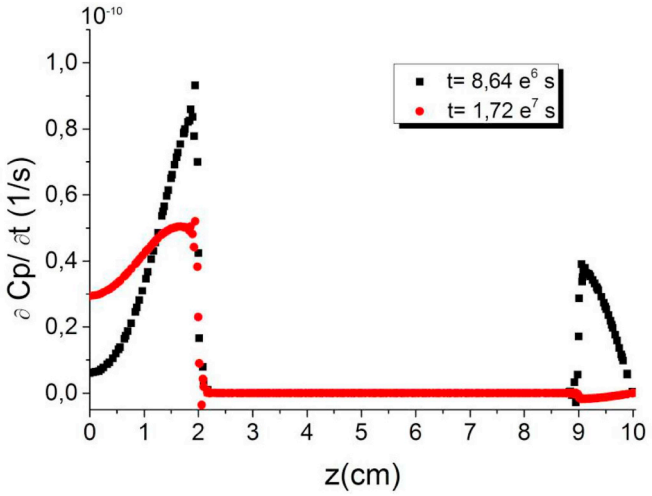

Fig. 12. Kinetic adsorption for three layer porous media (at t = 100 days and *t* = 200 days).

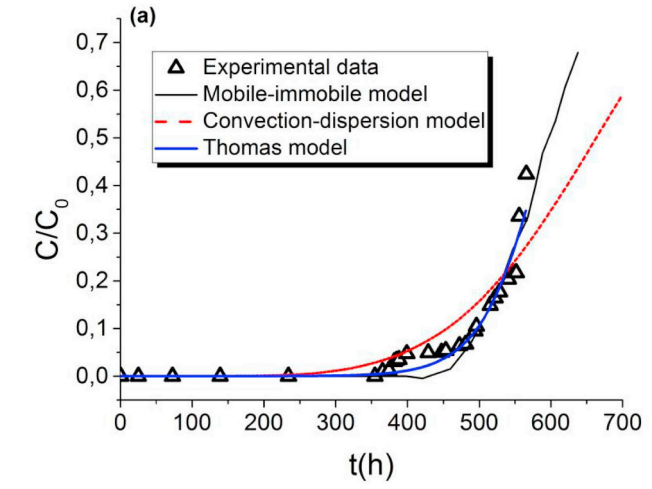

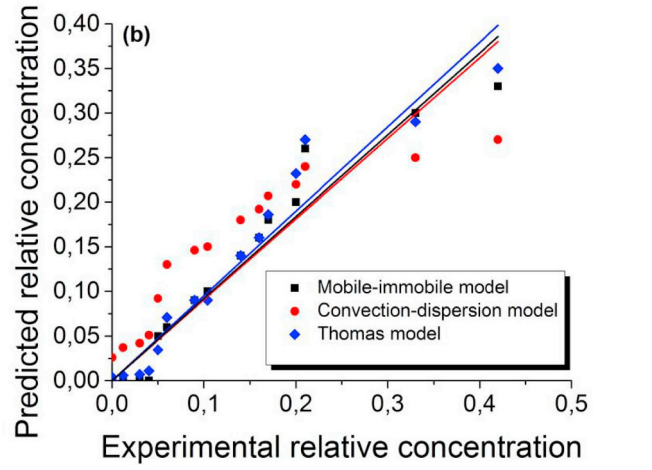

Fig. 13. (a). Comparison between simulated (lines) and measured for Exp C (symbols) MB relative concentration. Solid lines correspond to MIM model and dashed lines correspond to CDE model. (b). Predicted data from three models against experimental data of MB transport in silty soil.

Table 5
Determination coefficient and Error analysis of three models of the MB breakthrough curve.

	MIM	CDE	Thomas
R^2	0.9709	0.89	0.9704
E (%)	6	30.4	38

asymmetric, causing a significant adjustment error for the convection-dispersion-adsorption model. However, MIM model better reproduced the exponential shape profile with long tails (Table 5). This means the existence of an immobile water fraction in the porous medium.

4.5. Parameter sensitivity analysis

After MIM model validation, a parameter sensitivity analysis of this model on the MB breakthrough curve was performed. The MB transport is dominated by convection phenomena, dispersion, diffusion and adsorption in the presence of a mobile water fraction.

4.5. 1. Effect of the exchange coefficient

When the solute transfer coefficient (α) between the mobile and immobile fraction f of the liquid phase increases the increasing part of the breakthrough curve tends to be asymmetrical and spreads a long period (Fig. 14). Indeed, the more the breakthrough curves are asymmetrical the more exchange between mobile water and immobile water is important. Note also that the more the fraction f is close to 1 the more the model's sensitivity on this exchange coefficient is low. If the exchange coefficient α is very small, the solute velocity in the mobile fraction and transfer can be considered by the convection-dispersion but at a higher velocity than the convection-dispersion-adsorption model. However, an increase of the coefficient causes a rapid exchange and a tendency to have uniformity of the concentration in the two fractions of water which causes spreading of the breakthrough curve. Increasing degree of saturation of the medium and the pore velocity generates increased mobile water fraction and therefore the coefficient (Padilla et al., 1999). Nevertheless, there is no expressive relationship between f and α and between f and λ (Pang and Close, 1999) but an intense inverse correlation between α and λ.

4.5.2. Effect of longitudinal dispersivity

The influence of the local dispersivity does not make sense for low values of Peclet numbers that is to say to the low velocity. The increase in dispersivity causes an increase in dispersion coefficient, and thereafter, increasing mass diffusive flow and exchange between the mobile

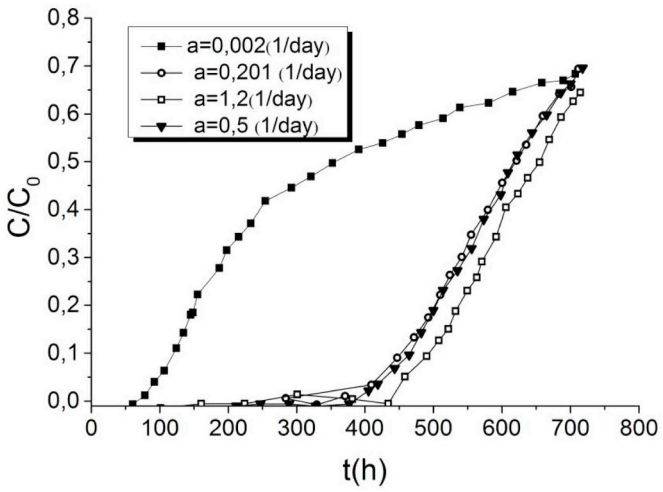

Fig. 14. Sensitivity of the MIM model to exchange coefficient.

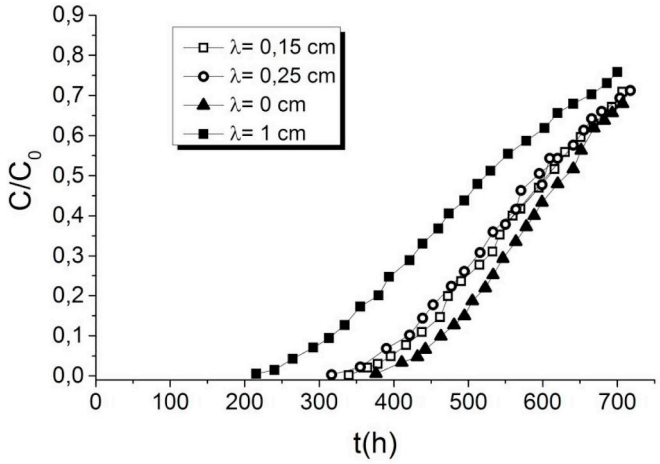

Fig. 15. Sensitivity of the MIM model to *longitudinal dispersivity*.

and immobile water regions. In our case, the flow velocity in the silty soil is low and thereafter a wide variation in the dispersion coefficient has no particular effect on the values breakthroughs concentrations (see Fig. 15).

4.5. 3. Effect of the diffusion coefficient

Fig. 16 shows the influence of a diffusion coefficient variation on the MB breakthrough curve. Indeed, by reducing the diffusion coefficient, the breakthrough curve becomes more spread out with a delay time of breakthrough, while an increase in this coefficient favors the transport of MB and causes rapid penetration of MB. So the effect of this factor is most evident in MB breakthrough time (a small influence on the concentration value (y-axis)).

4.5. 4. Effect of the distribution coefficient

A variation of this parameter has an impact on the amplitude change and an offset in the time of the simulated curve. The breakthrough curve is quite sensitive to a variation in distribution coefficient (Fig. 17). Indeed, an increase of this coefficient resulted in a delay output of the solution (a significant increase of breakthrough time), a spreading of the breakthrough curve and a decrease in the outlet concentration. By increasing this coefficient, the solid matrix retains and traps the material and, thereafter, it delays the transfer. The variation of distribution coefficient causes a variation in time required to reach the equilibrium (Musielak, 2012). Thereafter, this coefficient is involved as a term of delay.

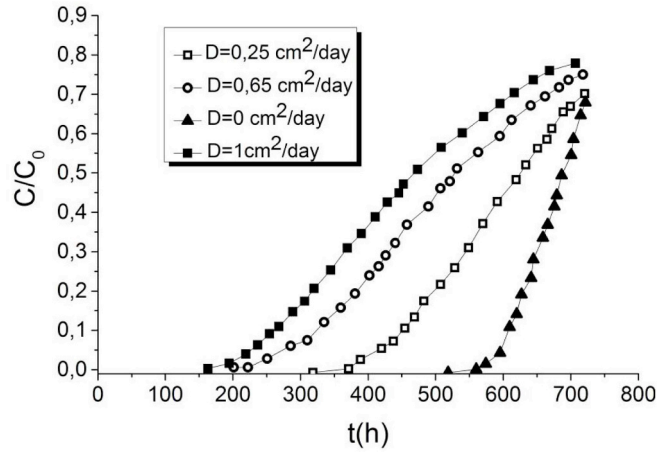

Fig. 16. Sensitivity of the MIM model to diffusion coefficient.

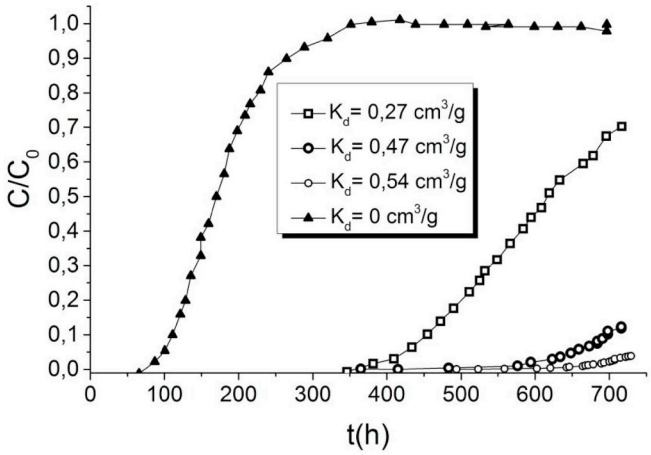

Fig. 17. Sensitivity of the MIM model to distribution coefficient.

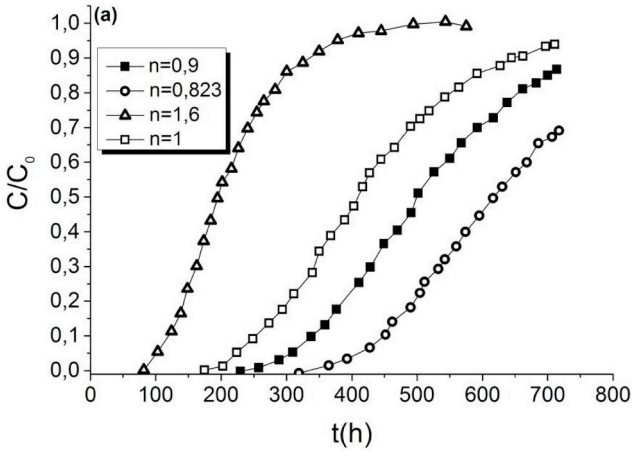

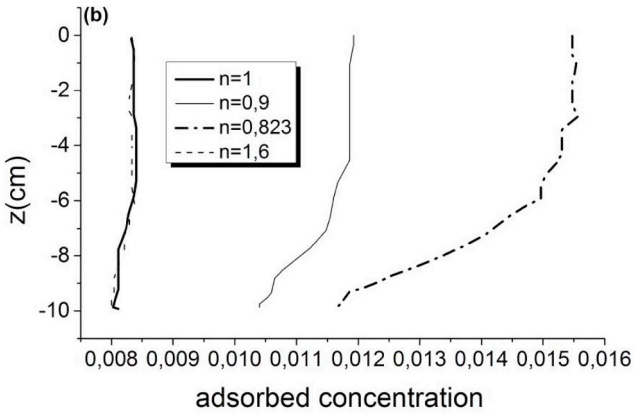

Fig. 18. (a). MIM model sensitivity to the Freundlich coefficient, (b) Profiles of adsorbed concentration for different values of the Freundlich coefficient.

4.5. 5. Effect of the Freundlich coefficient

Fig. 18 represents the breakthrough curves for different values of Freundlich coefficient (n). It is noted that the relative concentration increases with increasing Freundlich coefficient unlike the concentration of MB adsorbed on the soil grains. For $n = 1$ (linear isotherm) or $n > 1$, the delay coefficient is low and the breakthrough curve becomes symmetrical. This symmetry decreases with the decrease of n that is to means higher the coefficient n decreases as the curve becomes non-linear. In the case of a non-linear isotherm ($n < 1$) the concentration of MB in the liquid phase decreases proportionally with decreasing

Freundlich coefficient (Fig. 18(a)) which is not the case for the MB adsorbed concentration on the solid phase. In fact, for $n = 0.823$ a decrease in the MB concentration in the liquid phase (compared to the case of the linear isotherm ($n = 1$)) was found. This decrease leads to an increase of the delay coefficient, which causes an increase in adsorbed concentration on the solid phase. At equilibrium and for nonlinear adsorption, the adsorption is more significant and the delay dispersion and are stronger and the shape of the elution curve is asymmetrical (Fig. 18 (b)).

5. Conclusion

The aim of this work was to study the MB adsorption in layered soil and to discuss the effectiveness of layered soil in the reduction of organic pollutant transport. The results showed that the adsorption isotherm is described using Langmuir model for sand and Freundlich model for clay and silty soil. Also, the adsorption kinetic is described using pseudo first order model for both materials (sand and clay) and pseudo second order for silty soil. Both the experimental exploration and the numerical simulation showed that the three-layer capillary barrier cover system performs as inhibitor to minimize pollutant percolation. Therefore, in capillary barrier, the MB kinetic adsorption is inversely proportional to the flow velocity. The comparative analysis between three models proved that mobile-immobile model is the suitable one to describe the adsorption and transport of MB in unsaturated soil.

References

Abdelkawy, M.A., Zaky, M.A., Bhrawy, A.H., Baleanu, D., 2015. Numerical simulation of time variable fractional order mobile-immobile advection-dispersion model. Rom. Rep. Phys. 67 (3), 1–19.

AFNOR, NF X 31–130 soil quality, 1999. Chemical Methods, Determination of Cation Exchange Capacity (CEC) and Cation Extraction. AFNOR, Paris.

Arab, P.B., Araújo, T.P., Pejon, O.J., 2015. Identification of clay minerals in mixtures subjected to differential thermal and thermogravimetry analyses and methylene blue adsorption tests. Appl. Clay Sci. 114, 133–140.

Aubertin, M., Cifuentes, E., Apithy, S.A., Bussière, B., Molson, J., Chapuis, R.P., 2009. Analyses of water diversion along inclined covers with capillary barrier effects. Can. Geotech. J. 46 (10), 1146–1164.

Auta, M., Hameed, B.H., 2014. Chitosan–clay composite as highly effective and low-cost adsorbent for batch and fixed-bed adsorption of methylene blue. Chem. Eng. J. 237, 352–361.

Berkowitz, B., Cortis, A., Dentz, M., Scher, H., 2006. Modeling non-Fickian transport in geological formations as a continuous time random walk. Rev. Geophys. 44 (2), .

Bijeljic, B., Raeini, A., Mostaghimi, P., Blunt, M.J., 2013. Predictions of non-Fickian solute transport in different classes of porous media using direct simulation on pore-scale images. Phys. Rev. 530 87 (1), 013011.

Bradford, S.A., Simunek, J., Bettahar, M., van Genuchten, M.T., Yates, S.R., 2003. Modeling colloid attachment, straining, and exclusion in saturated porous media. Environ. Sci. Technol. 37 (10), 2242–2250 .

Chen, C., Gunawan, P., Xu, R., 2011. Self-assembled Fe 3 O 4-layered double hydroxide colloidal nanohybrids with excellent performance for treatment of organic dyes in water. J. Mater. Chem. 21 (4), 1218–1225.

Christie, R., 2001. Colour Chemistry. Royal Society of Chemistry.

Cortis, A., Harter, T., Hou, L., Atwill, E.R., Packman, A.I., Green, P.G., 2006. Transport of Cryptosporidium parvum in porous media: long-term elution experiments and continuous time random walk filtration modeling. Water Resour. Res. 42 (12), .

Cremer, C.J., Neuweiler, I., Bechtold, M., Vanderborght, J., 2016. Solute transport in heterogeneous soil with time-dependent boundary conditions. Vadose Zone J. 15 (6), .

Drummond, J.D., Aubeneau, A.F., Packman, A.I., 2014. Stochastic modeling of fine particulate organic carbon dynamics in rivers. Water Resour. Res. 50 (5), 4341–4356.

Fang, J., Xu, M.J., Wang, D.J., Wen, B., Han, J.Y., 2013. Modeling the transport of TiO2 nanoparticle aggregates in saturated and unsaturated granular media: effects of ionic strength and pH. Water Res. 47 (3), 1399–1408.

Ferencz, L., Balog, A., 2010. A pesticide survey in soil, water and foodstuffs from central Romania. Carpath. J. Earth Env. Sci. 5 (1), 111–118.

Flury, M., Wai, N.N., 2003. Dyes as tracers for vadose zone hydrology. Rev. Geophys. 41 (1).

Freundlich, H.M.F., 1906. Over the adsorption in solution. J. Phys. Chem. 57 (385471), 1100–1107.

Fujimaki, H., Inoue, M., 2003. A transient evaporation method for determining soil hydraulic proprieties at low pressure. Vadose Zone J. 2, 400–408.

Gimbert, F., Morin-Crini, N., Renault, F., Badot, P.M., Crini, G., 2008. Adsorption isotherm models for dye removal by cationized starch-based material in a single component system: error analysis. J. Hazard Mater. 157 (1), 34–46.

Harnas, F.R., Rahardjo, H., Leong, E.C., Wang, J.Y., 2014. Experimental study on dual capillary barrier using recycled asphalt pavement materials. Can. Geotech. J. 51 (10), 1165–1177.

Hethnawi, A., Nassar, N.N., Manasrah, A.D., Vitale, G., 2017. Polyethylenimine-functionalized pyroxene nanoparticles embedded on Diatomite for adsorptive removal of dye from textile wastewater in a fixed-bed column. Chem. Eng. J. 320, 389–404.

Khire, M.V., Benson, C.H., Bosscher, P.J., 2000. Capillary barriers: design variables and water balance. J. Geotech. Geoenviron. Eng. 126 (8), 695–708.

Kumar, K.V., Ramamurthi, V., Sivanesan, S., 2005. Modeling the mechanism involved during the sorption of methylene blue onto fly ash. J. Colloid Interface Sci. 284 (1), 14–21.

Kumar, A., Sharma, A.K., Rani, A., 2015. Transport of solutes under transient flow conditions–A case study–Yamuna river sub basin (Kosi Kalan to Agra). International Soil and Water Conservation Int. Soil Water Conserv. Res. 3 (3), 209–223.

Langmuir, I., 1918. Adsorption of gases on plain surfaces of glass mica platinum. J. Am. Chem. Soc. 40, 1361–1403.

Li, J.H., Du, L., Chen, R., Zhang, L.M., 2013. Numerical investigation of the performance of covers with capillary barrier effects in South China. Comput. Geotech. 48, 304–315.

Li, X., Chen, H., Jiang, X., Yu, Z., Yao, Q., 2017. Impacts of human activities on nutrient transport in the Yellow River: the role of the water-sediment regulation scheme. Sci. Total Environ. 592, 161–170.

Liang, L., Ju, L., Hu, J., Zhang, W., Wang, X., 2016. Transport of sodium dodecylbenzene sulfonate (SDBS)-dispersed carbon nanotubes and enhanced mobility of tetrabromobisphenol A (TBBPA) in saturated porous media. Colloid. Surface. Physicochem. Eng. Aspect. 497, 205–213.

Malik, A., Grohmann, E. (Eds.), 2011. Environmental Protection Strategies for Sustainable Development.

Mall, I.D., Srivastava, V.C., Agarwal, N.K., Mishra, I.M., 2005. Removal of Congo red from aqueous solution by bagasse fly ash and activated carbon: kinetic study and equilibrium isotherm analyses. Chemosphere 61 (4), 492–501.

Mancarella, D., Doglioni, A., Simeone, V., 2012. On capillary barrier effects and debris slide triggering in unsaturated layered covers. Eng. Geol. 147, 14–27.

Moslehi, M., de Barros, F.P., 2017. Uncertainty quantification of environmental performance metrics in heterogeneous aquifers with long-range correlations. J. Contam. Hydrol. 196, 21–29.

Musielak, M., 2012. Etude numérique et expérimentale des transferts de Composés Organiques Volatils du sol à l'air ambiant, en passant au travers du béton. Doctoral dissertation. Institut National Polytechnique de Toulouse-INPT.

Neuman, S.P., Tartakovsky, D.M., 2009. Perspective on theories of non-Fickian transport in heterogeneous media. Adv. Water Resour. 32 (5), 670–680.

Ng, C.W., Liu, J., Chen, R., Xu, J., 2015. Physical and numerical modeling of an inclined three-layer (silt/gravelly sand/clay) capillary barrier cover system under extreme rainfall. Waste Manag. 38, 210–221.

Padilla, I.Y., Yeh, T.J., Conklin, M.H., 1999. The effect of water content on solute transport in unsaturated porous media. Water Resour. Res. 35 (11), 3303–3313.

Pandey, A.K., Kumar, R., Singh, M.K., 2018. Solution to advection–dispersion equation for the heterogeneous medium using Duhamel's principle. In: Applications of Fluid Dynamics. Springer, Singapore, pp. 559–571.

Pang, L., Close, M., 1999. Field-scale physical non-equilibrium transport in an alluvial gravel aquifer. J. Contam. Hydrol. 38 (4), 447–464.

Parker, J.C., van Genuchten, M.Th, 1984. Flux-averaged and volume-averaged concentrations in continuum approaches to solute transport. Water Resour. Res. 20, 866e872.

Pedretti, D., Fernàndez-Garcia, D., Sanchez-Vila, X., Bolster, D., Benson, D.A., 2014. Apparent directional mass-transfer capacity coefficients in three-dimensional anisotropic heterogeneous aquifers under radial convergent transport. Water Resour. Res. 50 (2), 1205–1224.

Predelus, D., Coutinho, A.P., Lassabatere, L., Bien, L.B., Winiarski, T., Angulo-Jaramillo, R., 2015. Combined effect of capillary barrier and layered slope on water, solute and nanoparticle transfer in an unsaturated soil at lysimeter scale. J. Contam. Hydrol. 181, 69–81.

Reddy, P.M.K., Mahammadunnisa, S.K., Ramaraju, B., Sreedhar, B., Subrahmanyam, C., 2013. Low-cost adsorbents from bio-waste for the removal of dyes from aqueous solution. Environ. Sci. Pollut. Res. 20 (6), 4111–4124.

Rumynin, V.G., 2012. Subsurface Solute Transport Models and Case Histories: with Applications to Radionuclide Migration, vol. 25 Springer Science & Business Media, .

Sadeghi, M., Tuller, M., Gohardoust, M.R., Jones, S.B., 2014. Column-scale unsaturated hydraulic conductivity estimates in coarse-textured homogeneous and layered soils derived under steady-state evaporation from a water table. J. Hydrol. 519, 1238–1248.

Sana, D., Jalila, S., 2016. Combined effect of unsaturated soil condition and soil heterogeneity on methylene blue adsorption/desorption and transport in fixed bed column: experimental and modeling analysis. J. King Saud Univ. Sci. 28 (4), 308–317.

Schindler, U., Durner, W., von Unold, G., Muller, L., 2010. Evaporation Method for estimating measuring unsaturated hydraulic properties of soils: extending the measurement range. Soil Physics 74, 1071–1083.

Simunek, J., Wenderworth, O., van Genuchten, M. Th, 1998. Parameter estimation analysis of the evaporation method for determining soil hydraulic properties. Soil Sci. Soc. Am. J. 62, 894–905.

Song, B., Xu, P., Zeng, G., Gong, J., Wang, X., Yan, J., et al., 2018. Modeling the transport of sodium dodecyl benzene sulfonate in riverine sediment in the presence of multi-walled carbon nanotubes. Water Res. 129, 20–28.

Stein, A., Droogers, P., Booltink, H., 1998. Point processes and random sets for analyzing patterns of methylene blue coloured soil. Soil. Till. Res. 46 (3), 273–288.

Suter, G.W., Luxmoore, R.J., Smith, E.D., 1993. Compacted soil barriers at abandoned landfill sites are likely to fail in the long term. J. Environ. Qual. 22 (2), 217–226.
Thomas, C.H., 1944. Heterogeneous ion exchange in a flowing system, 793. J. Am. Chem. Soc. 66 (2), 1664–1666.
Torkzaban, S., Bradford, S.A., van Genuchten, M.T., Walker, S.L., 2008. Colloid transport in unsaturated porous media: the role of water content and ionic strength on particle straining. J. Contam. Hydrol. 96 (1), 113–127.
Van Genuchten, M.Th, Wierenga, P.J., 1976. Mass transfer studies in sorbing porous media I. Analytical solutions. Soil Sci. Soc. Am. J. 40, 473–480.
Wang, D., Bradford, S.A., Harvey, R.W., Hao, X., Zhou, D., 2012. Transport of ARS-labeled hydroxyapatite nanoparticles in saturated granular media is influenced by surface charge variability even in the presence of humic acid. J. Hazard Mater. 229, 170–176.
Wawrzkiewicz, M., Hubicki, Z., 2009. Kinetic studies of dyes sorption from aqueous solutions onto the strongly basic anion-exchanger Lewatit MonoPlus M-600. Chem. Eng. J. 150 (2), 509–515.
Wessolek, G., Plagge, R., Leij, F.J., van Genuchten, M. Th, 1994. Analysing problems in describing field and laboratory measured soil hydraulic properties. Geoderma 64, 93–110.
Yukselen, Y., Kaya, A., 2008. Suitability of the methylene blue test for surface area, cation exchange capacity and swell potential determination of clayey soils. Eng. Geol. 102 (1), 38–45.